

of this epitope by a highly conserved mitotic regulator, Pin1.

Our results suggest a two-step mechanism for mitotic regulation. Phosphorylation at specific S/T-P sites by mitotic kinases creates a binding site for Pin1, which, in turn, induces conformational changes by catalyzing prolyl isomerization (Fig. 3). Such local conformational changes could alter the activity of a phosphoprotein such as NIMA (4) or Cdc25 (7), its ability to interact with other proteins, or its degradation. In this manner, Pin1 would provide an additional posttranslational level of control, allowing the general increase in protein phosphorylation to result in the organized and programmed set of structural modifications that occur during mitosis. Given that inhibition of Pin1 induces mitotic arrest and apoptosis (4), this Pin1-mediated mechanism is a potential therapeutic target for cancer.

REFERENCES AND NOTES

1. P. Nurse, *Cell* **79**, 547 (1994); R. W. King, P. K. Jackson, M. W. Kirschner, *ibid.*, p. 563; T. R. Coleman and W. G. Dunphy, *Curr. Opin. Cell Biol.* **6**, 877 (1994).
2. E. A. Nigg, *Bioessays* **17**, 471 (1995).
3. R. Heald and F. McKeon, *Cell* **61**, 579 (1990); E. Bally *et al.*, *Nature* **350**, 715 (1991); A. Blangy *et al.*, *Cell* **83**, 1159 (1995).
4. K. P. Lu, S. D. Hanes, T. Hunter, *Nature* **380**, 544 (1996); K. P. Lu and T. Hunter, *Cell* **81**, 413 (1995).
5. S. L. Schreiber, *Science* **251**, 283 (1991); G. Fischer, *Angew. Chem. Int. Ed. Engl.* **33**, 1415 (1994); F. X. Schmid, *Curr. Biol.* **5**, 993 (1995).
6. J. U. Rahfeld *et al.*, *FEBS Lett.* **352**, 180 (1994); *ibid.* **343**, 65 (1994); K. E. Rudd *et al.*, *Trends Biochem. Sci.* **20**, 12 (1995).
7. M. Shen, P. T. Stukenberg, M. W. Kirschner, K. P. Lu, in preparation.
8. The oriented peptide library approach [Z. Songyang *et al.*, *Cell* **72**, 767 (1993)] was used to screen for optimal peptides. All amino acids except Cys were incorporated in equimolar amounts at each degenerate position, yielding a total theoretical degeneracy for each library of 19^9 (4.7×10^7) distinct peptide sequences. GST-Pin1-conjugated beads, or MPM-2 antibody bound to protein G-conjugated beads, were incubated with the peptide library mixtures and then washed extensively. Bound peptides were eluted with 30% (v/v) acetic acid and sequenced.
9. R. Ranganathan, K. P. Lu, T. Hunter, J. P. Noel, *Cell* **89**, 875 (1997).
10. Chromogenic oligopeptides were synthesized [A. Bernhardt, M. Drewello, M. Schutkowski, *Int. J. Pept. Protein Res.* **50**, 143 (1997)], and their sequences were confirmed by nuclear magnetic resonance. Standard peptides were obtained from Bachem. PPlase activity was assayed, and the bimolecular rate constant (k_{cat}/K_m) was calculated according to the equation $k_{cat}/K_m = (k_{obs} - k_u)/[PPlase]$, where [PPlase] is the concentration of PPlase, k_u is the first-order rate constant for spontaneous cis-trans isomerization, and k_{obs} is the pseudo-first-order rate constant for cis-trans isomerization in the presence of PPlase, as described [G. Fischer, H. Bang, C. Mech, *Biomed. Biochim. Acta* **43**, 1101 (1984); J. L. Kofron *et al.*, *Biochemistry* **30**, 6127 (1991)]. The affinity of Pin1 for peptides was measured as described [M. Schutkowski, S. Wöllner, G. Fischer, *Biochemistry* **34**, 13016 (1995)].
11. M. B. Yaffe *et al.*, data not shown.
12. Molecular model-building was based on the coordinates of the Pin1 structure (9). The phosphate of pS in the modeled peptide was superimposed on the cocrystallizing sulfate ion in the original Pin1

structure, and Pro residue displacements were minimized with respect to the Ala-Pro ligand in the original Pin1 structure. Figures were made with the programs GRASP [A. Nicholls, K. Sharp, B. Honig, *Proteins* **11**, 281 (1991)], Molscript, and Raster3d.

13. Point mutations were introduced into Pin1 by polymerase chain reaction-based techniques and verified by DNA sequencing. The mutant proteins were expressed and purified as described (4, 7).
14. For Pin1, the ratio of k_{cat}/K_m values for the phosphorylated versus unphosphorylated substrates is 19,400/7, which is about equal to the ratio of 1120/<1 for the H59A mutant.
15. The protein sequence database was screened with the use of the program INDOVINATOR (S. Volinia, J. Lai, L. Cantley, in preparation), with an entropy-based weighting technique to score for relative information content at each amino acid position flanking the pS/pT-P motif with the quantitative peptide library results, which are shown qualitatively in Table 3 (see www.sciencemag.org/feature/data/974519.shl).
16. J. Kuang *et al.*, *Mol. Biol. Cell* **5**, 135 (1994); X. S. Ye *et al.*, *EMBO J.* **14**, 986 (1995); T. Izumi, D. H. Walker, J. L. Maller, *Mol. Biol. Cell* **3**, 927 (1992); A.

Kumagai and W. G. Dunphy, *Science* **273**, 1377 (1996).

17. Lysates of interphase and mitotic HeLa cells were incubated with GST or GST-Pin1 beads and the precipitated proteins subjected to immunoblot analysis with various antibodies, as described (7). S6 kinase antibodies are from N. Terada (National Jewish Medical and Research Center) and Upstate Biotechnology and Rab4 antibodies are from Santa Cruz Biotechnology.
18. S. D. Hanes *et al.*, *Yeast* **5**, 55 (1989); R. Maleszka *et al.*, *Proc. Natl. Acad. Sci. U.S.A.* **93**, 447 (1996).
19. F. M. Davis *et al.*, *Proc. Natl. Acad. Sci. U.S.A.* **80**, 2926 (1983); J. M. Westendorf, P. N. Rao, L. Gerace, *ibid.* **91**, 714 (1994); S. Taagepera *et al.*, *Mol. Biol. Cell* **5**, 1243 (1994).
20. We thank M. Berne, A. Bernhardt, and B. Hökelmann for peptide synthesis and sequencing and N. Terada for the antibodies to S6 kinase. M.B.Y. is a Howard Hughes Physician-Scientist Fellow. Supported by Deutsche Forschungsgemeinschaft, Fonds der Chemischen Industrie, and Boehringer Ingelheim Stiftung to G.F., and NIH grants GM56203 to L.C.C. and GM56230 to K.P.L.

18 August 1997; accepted 3 November 1997

Mechanism of Transcription Through the Nucleosome by Eukaryotic RNA Polymerase

Vasily M. Studitsky,* George A. Kassavetis, E. Peter Geiduschek, Gary Felsenfeld†

Nucleosomes, the nucleohistone subunits of chromatin, are present on transcribed eukaryotic genes but do not prevent transcription. It is shown here that the large yeast RNA polymerase III transcribes through a single nucleosome. This takes place through a direct internal nucleosome transfer in which histones never leave the DNA template. During this process, the polymerase pauses with a pronounced periodicity of 10 to 11 base pairs, which is consistent with restricted rotation in the DNA loop formed during transfer. Transcription through nucleosomes by the eukaryotic enzyme and by much smaller prokaryotic RNA polymerases thus shares many features, reflecting an important property of nucleosomes.

Many transcribed genes are covered with nucleosomes (1, 2), which raises the question of how the polymerase negotiates its obstructed passage (3, 4). When the bacteriophage SP6 RNA polymerase transcribes through the nucleosome, the histone octamer steps around the polymerase by forming an intranucleosomal DNA loop (5). The looped intermediate causes intermittent pausing during the advance of the polymerase (6). Here we show that this mechanism is also relevant for eukaryotic RNA polymerases.

The ability of eukaryotic RNA poly-

merases to transcribe chromatin templates in vitro has been demonstrated (7–13), but the mechanism of transcription through the nucleosome remains obscure. Here we describe a new system for comparing transcription of identical nucleosomal templates by phage SP6 RNA polymerase and yeast RNA polymerase III (Pol III).

The template used for transcription was a 227-base pair (bp) Sac I–Nco I fragment (5) containing a positioned nucleosome and an SP6 promoter (Fig. 1A). DNA and nucleosomal templates labeled at the Nco I end were transcribed for different lengths of time (Fig. 1B). Elongation complexes were formed on DNA and nucleosomal templates with similar efficiency (on 25 to 30% of the templates). When elongation was continued for 5 min, the intensity of the low-mobility band was substantially reduced, which suggests that transcription on a majority of the templates was completed. Quantitative recovery of label from the elongation complexes in the nucleosomal band (naked DNA

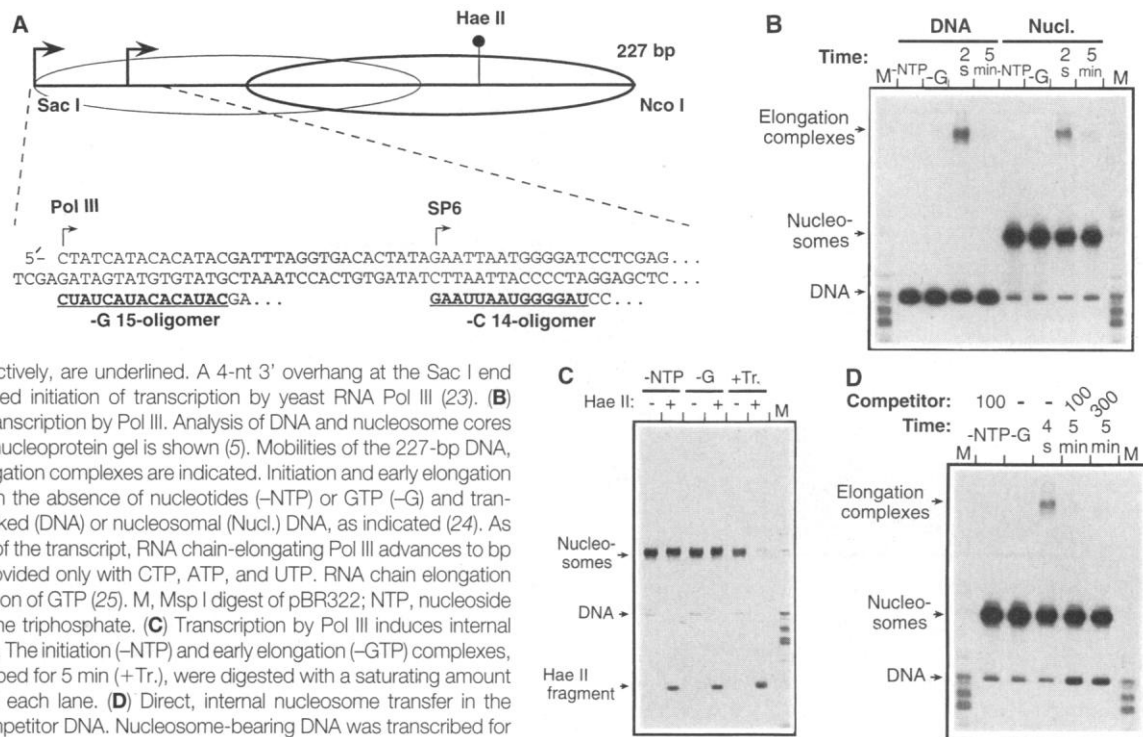
V. M. Studitsky and G. Felsenfeld, Laboratory of Molecular Biology, National Institute of Diabetes and Digestive and Kidney Diseases, National Institutes of Health, Bethesda, MD 20892, USA.

G. A. Kassavetis and E. P. Geiduschek, Department of Biology and Center for Molecular Genetics, University of California, San Diego, La Jolla, CA 92093–0634, USA.

*Present address: Department of Biochemistry and Molecular Biology, Wayne State University School of Medicine, 540 East Canfield Avenue, Detroit, MI 48201, USA.

†To whom correspondence should be addressed.

Fig. 1. Analysis of the fate of nucleosomes on transcription by Pol III. **(A)** The 227-bp Sac I–Nco I template. The principal positions of the nucleosome core before (bold oval) and after transcription (light oval) are indicated. Initiation sites for yeast Pol III and phage SP6 RNA polymerases are indicated, and sequences of RNA synthesized in the absence of GTP or CTP, respectively, are underlined. A 4-nt 3' overhang at the Sac I end promotes efficient end-directed initiation of transcription by yeast RNA Pol III (23). **(B)** Nucleosomes re-form after transcription by Pol III. Analysis of DNA and nucleosome cores labeled at the Nco I end in a nucleoprotein gel is shown (5). Mobilities of the 227-bp DNA, nucleosomes, and Pol III elongation complexes are indicated. Initiation and early elongation complexes were performed in the absence of nucleotides (–NTP) or GTP (–G) and transcribed for 2 s or 5 min on naked (DNA) or nucleosomal (Nucl.) DNA, as indicated (24). As there is no G in the first 15 nt of the transcript, RNA chain-elongating Pol III advances to bp 15 and then arrests when provided only with CTP, ATP, and UTP. RNA chain elongation resumes promptly upon addition of GTP (25). M, Msp I digest of pBR322; NTP, nucleoside triphosphates; GTP, guanosine triphosphate. **(C)** Transcription by Pol III induces internal transfer of a nucleosome core. The initiation (–NTP) and early elongation (–GTP) complexes, as well as complexes transcribed for 5 min (+Tr.), were digested with a saturating amount of Hae II as indicated above each lane. **(D)** Direct, internal nucleosome transfer in the presence of an excess of competitor DNA. Nucleosome-bearing DNA was transcribed for 4 s in the absence, or for 5 min in the presence, of unlabeled competitor DNA (final concentrations are indicated in micrograms per milliliter). Nucleosome cores were formed and analyzed as described (5); they were pre-digested with Hae II restriction enzyme (26) and purified in preparative nucleoprotein gel (6). Yeast RNA Pol III was purified as described (27).



was not generated) suggested that nucleosomes survive transcription by Pol III.

Does the position of the nucleosome core change during transcription? Positions of nucleosomes before and after transcription were analyzed with a restriction enzyme assay [Fig. 1C (5, 11)]. Only ~20% of nucleosomes were sensitive to digestion in the presence of Hae II restriction endonuclease before transcription, which indicates that most nucleosomes were positioned at the Nco I end. In contrast, the sensitivity of most nucleosome cores to this enzyme after transcription indicated quantitative transfer to the Sac I end. The amount of label in the free-DNA band did not increase after transfer. In contrast, ~10% of nucleosomes fall apart on transcription by the SP6 polymerase (5), which suggests that Pol III–dependent transfer of the histone octamer is more efficient.

The mobility of a nucleosome in the gel indicates its position on a DNA fragment with ~10-bp resolution; nucleosomes positioned symmetrically about the fragment center have the same mobility (14, 15). Therefore, the very similar mobilities of nucleosomes before and after transcription indicate transfer from the Nco I end to the Sac I end of the fragment over a distance of ~80 bp, which is very similar to the distance of transfer when SP6 polymerase transcribes the same template (5).

Is the histone octamer transferred within the same DNA molecule? Labeled nucleosomes were transcribed in the presence of

excess unlabeled competitor DNA (Fig. 1D). The amount of free labeled DNA increased after transcription, indicating appreciable transfer of the histone octamer to unlabeled competitor DNA (5). However even in the presence of competitor DNA, 50 to 60% of the label from the elongation complexes was still recovered in the nucleosome band, which suggests relatively efficient nucleosome transfer by a direct mechanism within the same DNA molecule. In comparison, only ~30% of nucleosomes survived transcription by SP6 polymerase in the presence of competitor DNA (5), again suggesting more efficient internal nucleosome transfer than with SP6 polymerase.

The pace of transcription of naked DNA and nucleosomes by Pol III and SP6 RNA polymerase was also analyzed (Fig. 2). Both polymerases quickly completed transcripts on the naked DNA template. The broad size distribution of transcripts at early time points (2 and 4 s) has been analytically modeled in terms of the existence of two states of RNA polymerase at each step of RNA chain elongation: one competent to add the next nucleotide rapidly and the other not (16). Recent results suggest a structural interpretation of the elongation-blocked state: It arises when the RNA polymerase catalytic site moves out of register with the 3' end of the nascent transcript (17–19); if the RNA-DNA duplex and transcription bubble-shift concomitantly,

the growing point of the RNA chain disengages from the DNA template strand (17).

Nucleosomal templates slowed transcription, with SP6 and Pol III elongation complexes encountering obstruction predominantly within the promoter-proximal half of nucleosomal DNA. Nucleosome-generated obstructions to RNA chain elongation by Pol III were clustered, with an apparent periodicity of 10 to 11 nucleotides (nt) (Fig. 2C), generating peaks at about nt 105, 116, 126, and 137 after 4 s of RNA synthesis (Fig. 2A). Although some obstructions were transient (at nt 105 and 126), others persisted (at nt 116 and 137). Other transcripts (at nt 104, 140, 142, 147, and 150) were less identifiable with nucleosome-generated arrest; for example, the lack of an apparent precursor, and delayed appearance, of the nt 104 transcript points to events subsequent to obstruction of elongation. Although many transcripts were never completed during the allotted time (Fig. 2A), experiments with sarkosyl, which strips nucleosomes from DNA but leaves elongation complexes intact and able to complete nascent transcripts (20), indicated that at least 50% of obstructed polymerases were still functional at the last point of the time course (21).

The similarity of the Pol III– and SP6-specific pausing patterns strongly suggests that the same mechanism operates in both cases. This is surprising in view of the different sizes of the polymerases: Phage SP6 RNA polymerase is a small (~100 kD) single-subunit pro-

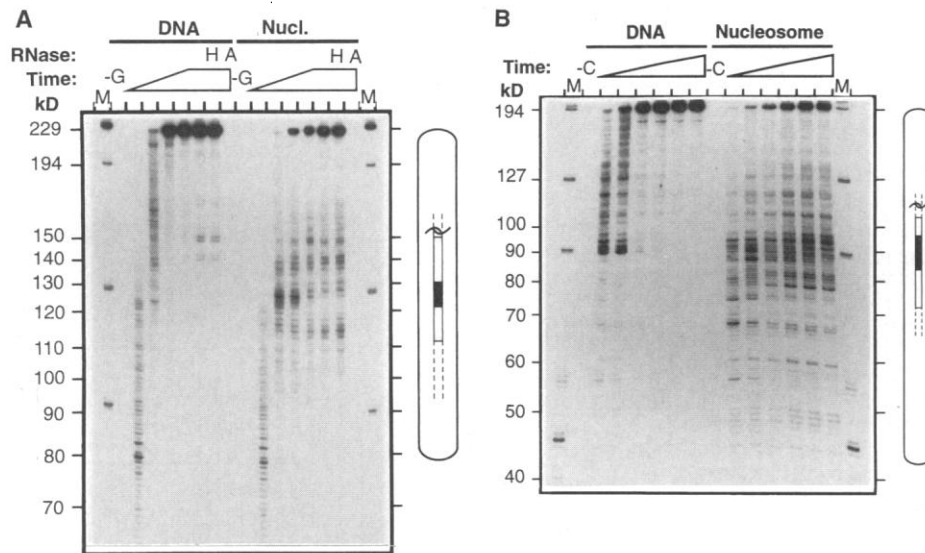


Fig. 2. Analysis of nucleosome-specific pausing. **(A)** Time courses of transcript elongation by Pol III on the 227-bp template (28). Analysis of transcripts on denaturing polyacrylamide gel electrophoresis is shown. Cores and 227-bp DNA were transcribed at 20°C for different times (from left to right: 2, 4, 8, 30, and 180 s) after formation of early elongation complexes (-G). Samples were also incubated with ribonuclease (RNase) A (A) or RNase H (H) as indicated after 180 s of transcription. Transcripts were sensitive to RNase A and resistant to RNase H, indicating no formation of extended DNA-RNA hybrids. The original position of the nucleosome core is shown in the inset at the right: The region of strong nucleosome-induced pausing is indicated by a black box, the regions of less intense pausing by shaded boxes, and the regions of weak pausing by dashed lines; the nucleosomal dyad is indicated. SP6 polymerase runoff transcripts derived from a mixture of different restriction digests of pD70 were used as RNA markers (M) (6) (sizes are indicated on the left). **(B)** Time courses of transcript elongation by SP6 polymerase. Cores were transcribed for 4, 10, 25, 60, 180, and 600 s at 0°C after formation of early (14-oligomer) elongation complexes (-C). **(C)** Schematic diagram of nucleosome-induced pausing of the Pol III and SP6 RNA polymerases on the 227-bp template. The pausing patterns (after 8 s of transcription by Pol III or 25 s of transcription by SP6 polymerase) are plotted as black bars with heights directly proportional to the intensities of the corresponding bands in the gel. Transcription by SP6 RNA polymerase was as described (5, 6).

karyotic enzyme whereas yeast Pol III is one of the large (~600 kD), multisubunit, eukaryotic nuclear RNA polymerases. If, as previously proposed, the intranucleosomal DNA loop prevents rotation of either RNA polymerase around DNA, then it must be broken to allow continued elongation (6). When this occurs, even the much larger eukaryotic polymerase can continue RNA elongation until the loop forms again, forcing the enzyme to pause once more. Obstruction by the nucleosome can also drive elongating Pol III into a relatively prolonged state of blocked elongation.

The similar distances of the nucleosome transfers and the similarity of the SP6 polymerase and Pol III pausing patterns strongly

suggest similar topographies of the transfer intermediates (Fig. 3). Why is the 10- to 11-bp periodicity of pausing prominent in the case of Pol III? It seems reasonable to propose that because of the much larger size of Pol III, the DNA loop only forms when the polymerase is positioned precisely on the outside of the loop; rotation of the Pol III molecule is almost completely restricted after the loop is formed. Because the rotational orientation of DNA is fixed by the remaining DNA-histone contacts, and if only one rotational orientation of the polymerase is favorable for formation of the loop, the transfer intermediates would be formed with the observed 10- to 11-bp periodicity. The much weaker period-

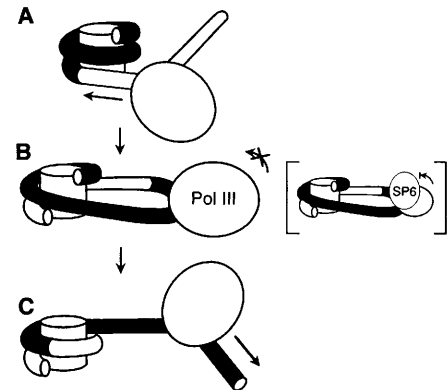


Fig. 3. A mechanism for transcription through a nucleosome. **(A)** RNA polymerase approaches the nucleosome. DNA in the elongation complex is severely bent (29); nucleosomal DNA is shaded. **(B)** A proposed structure of the transfer intermediate containing the intranucleosomal DNA loop. The relatively small size of the loop and the large size of Pol III result in transcriptional arrest with the observed 10-bp periodicity. In contrast, the much smaller SP6 RNA polymerase (right, in brackets) can continue to advance somewhat after loop formation. **(C)** Octamer transfer is completed.

icity in the case of SP6 polymerase may result from less severe restrictions on rotation of the smaller polymerase in the DNA loop. The smaller enzyme might be able to continue limited elongation (probably 2 to 5 nt) even after loop formation and might then stop only when it meets a DNA sequence intrinsically unfavorable for elongation.

Why is Pol III-induced transfer more efficient? The efficiency of SP6-dependent intramolecular nucleosome transfer is known to be greater at a lower elongation rate (5); the greater transfer efficiency by Pol III could be due to its intrinsically slower elongation rate.

What might be the consequences of direct transfer *in vivo*? Transcription would induce nucleosome translocation toward the promoter, depleting nucleosomes from the 3' end of the gene; of course, nucleosomes could be transferred back to this region (5). Thus, the nucleosomal organization of a transcribed gene should be dynamic (22).

Our results show clearly that a eukaryotic polymerase is capable of transcribing through a nucleosome without displacing it from the template. This ability reflects a property of nucleosomes that is likely to be of importance for the transcription process *in vivo*.

REFERENCES AND NOTES

1. M. Grunstein, *Annu. Rev. Cell Biol.* **6**, 643 (1990).
2. G. Felsenfeld, *Nature* **355**, 219 (1992).
3. D. Luse and G. Felsenfeld, in *Chromatin Structure and Gene Expression* (Oxford Univ. Press, New York, 1995), pp. 104-122.
4. F. Thoma, *Trends Genet.* **7**, 175 (1991).
5. V. M. Studitsky, D. J. Clark, G. Felsenfeld, *Cell* **76**, 371 (1994).
6. ———, *ibid.* **83**, 19 (1995).

NDR1, a Pathogen-Induced Component Required for Arabidopsis Disease Resistance

Karen S. Century,* Allan D. Shapiro,† Peter P. Repetti, Douglas Dahlbeck, Eric Holub, Brian J. Staskawicz‡

Plant disease resistance (*R*) genes confer an ability to resist infection by pathogens expressing specific corresponding avirulence genes. In *Arabidopsis thaliana*, resistance to both bacterial and fungal pathogens, mediated by several *R* gene products, requires the *NDR1* gene. Positional cloning was used to isolate *NDR1*, which encodes a 660–base pair open reading frame. The predicted 219–amino acid sequence suggests that *NDR1* may be associated with a membrane. *NDR1* expression is induced in response to pathogen challenge and may function to integrate various pathogen recognition signals.

Genetic analyses of disease resistance in plants show that resistance to pathogens is often highly specific, requiring single corresponding genetic loci in both the plant and the pathogen (1). Disease resistance genes cloned from diverse plant species such as tomato, rice, and *Arabidopsis thaliana* encode proteins that share one or more similar motifs (2). These motifs include leucine-rich repeat regions (implicated in protein-protein interactions) (3), nucleotide-binding sites, and kinase domains, all of which predict a role for resistance genes as components in signal transduction pathways. These genes confer resistance to a variety of pathogens, including bacteria, fungi, viruses, and nematodes, which suggests a conserved mechanism of plant disease resistance. Therefore, it is possible that the signal transduction pathways used by the different resistance gene products converge at some point. We report the cloning of *NDR1*

from *Arabidopsis*, a gene that functions in common among several resistance responses.

The *NDR1* locus is required for resistance to both the bacterial pathogen *Pseudomonas syringae* pv. *tomato* (*Pst*) and the fungal pathogen *Peronospora parasitica* (4). Mutation of *NDR1* causes susceptibility to numerous strains of these pathogens. Thus, *NDR1* represents a strong candidate for a conserved signal transduction element required for avirulence (*avr*) gene-specific disease resistance. *NDR1* is located on *Arabidopsis* chromosome three, in an ~8.5-centimorgan (cM) interval between restriction fragment length polymorphism (RFLP) markers *g6220* and *g4711* (4). Fine-structure mapping with RFLP and polymerase chain reaction (PCR)-based markers further delimited the genomic region carrying *NDR1* (Fig. 1A) (5). An overlapping set of yeast artificial chromosome (YAC) clones spanning ~1200 kb was constructed (Fig. 1B) (6). Two YAC clones, *CIC3D12* and *CIC7E1*, together spanned *NDR1*, as determined by recombination analysis. A plant-transformation competent cosmid library from each of these two YAC clones was generated, and a cosmid contig was constructed (Fig. 1C) (7). An approximate 1-kb deletion was uncovered in the *ndr1-1* fast-neutron-generated mutant (4) when cosmid FH6 from the *CIC3D12* library was

K. S. Century, A. D. Shapiro, P. P. Repetti, D. Dahlbeck, B. J. Staskawicz, Department of Plant and Microbial Biology, University of California, Berkeley, CA 94720–3102, USA. E. Holub, Plant Pathology and Weed Science Department, Horticulture Research International–Wellesbourne, Warwickshire CV35 9EF, UK.

*Present address: Biology Department, San Francisco State University, San Francisco, CA 94132, USA.

†Present address: Department of Plant and Soil Sciences, University of Delaware, Newark, DE 19717, USA.

‡To whom correspondence should be addressed. E-mail: stask@nature.berkeley.edu

Table 1. Asexual sporulation (measured as the mean number of sporangiophores per cotyledon; maximum of 20 sporangiophores counted per cotyledon) by three incompatible isolates of *Peronospora parasitica* on Col-0, the mutant *ndr1-1*, and two transformed lines of *ndr1-1*. *RPP* resistance specificities for each isolate are indicated. The cotyledon assay used has been described previously (31). SEM, standard error of the mean; n, number of seedlings inoculated.

Arabidopsis line	Peronospora isolate								
	Cala2-RPP2			Emwa1-RPP4			Emoy2-RPP4		
	Mean	SEM	(n)	Mean	SEM	(n)	Mean	SEM	(n)
Col-0	0.18	0.07	(76)	4.01	0.28	(86)	5.94	0.40	(58)
<i>ndr1-1</i>	0.95	0.11	(85)	10.54	0.57	(95)	14.66	0.60	(86)
<i>ndr1-1</i> FH6	0.03	0.03	(87)	4.89	0.29	(128)	7.00	0.41	(93)
<i>ndr1-1</i> CB17	0.69	0.10	(100)	10.91	0.53	(100)	14.03	0.62	(87)

7. J. C. Hansen and A. P. Wolfe, *Biochemistry* **31**, 7977 (1992).
8. S. A. Brown, A. N. Imbalzano, R. E. Kingston, *Genes Dev.* **10**, 1479 (1996).
9. B. ten Heggeler-Bordier, C. Schild-Poulter, S. Chapel, W. Wahli, *W. EMBO J.* **14**, 2561 (1995).
10. M. G. Izban and D. S. Luse, *Genes Dev.* **5**, 683 (1991).
11. R. H. Morse, *EMBO J.* **8**, 2343 (1989).
12. Y. Lorch, J. W. LaPointe, R. D. Kornberg, *Cell* **55**, 743 (1988).
13. R. Losa, and D. D. Brown, *ibid.* **50**, 801 (1987).
14. I. Duband-Goulet, V. Carot, A. V. Ulianov, S. Douc-Rasy, A. J. Prunell, *Mol. Biol.* **224**, 981 (1992).
15. G. Meersseman, S. Pennings, E. M. Bradbury, *EMBO J.* **11**, 2951 (1992).
16. H. Matsuzaki, G. A. Kassavetis, E. P. J. Geiduschek, *Mol. Biol.* **235**, 1173 (1994).
17. N. Komissarova and M. J. Kashlev, *J. Biol. Chem.* **272**, 15329 (1997).
18. R. Guajardo and R. J. Sousa, *Mol. Biol.* **265**, 8 (1997).
19. E. Nudler, A. Mustaev, E. Lukhtanov, A. Goldfarb, *Cell* **89**, 33 (1997).
20. J. A. Knezetic, G. A. Jacob, D. S. Luse, *Mol. Cell. Biol.* **8**, 3114 (1988).
21. V. M. Studitsky, G. A. Kassavetis, E. P. Geiduschek, G. Felsenfeld, data not shown.
22. D. J. Clark, in *The Nucleus*, A. Wolffe, Ed. (JAI Press, Greenwich, CT, 1995), pp. 207–239.
23. C. Bardeleben, G. A. Kassavetis, E. P. J. Geiduschek, *Mol. Biol.* **235**, 1193 (1994).
24. Initiation (–NTP) and early elongation (–GTP) complexes were not detected, probably because of instability during electrophoresis.
25. G. A. Kassavetis, D. L. Piggis, R. Negri, L. H. Nguyen, E. P. Geiduschek, *Mol. Cell. Biol.* **9**, 2551 (1989).
26. To isolate nucleosomes positioned at the Nco I end, reconstitutes were incubated in the presence of 10 U of Hae II restriction enzyme in SP6 transcription buffer at 20°C for 45 min and separated from free DNA and differently positioned cores in preparative nucleoprotein gels.
27. G. A. Kassavetis, B. R. Braun, L. H. Nguyen, E. P. Geiduschek, *Cell* **60**, 235 (1990).
28. Transcription by yeast RNA Pol III proceeded in one of two ways. For experiments with labeled RNA, elongation complexes arrested before the first G were formed by incubation of 10 ng of template DNA (cores or free DNA) in 20 μl of transcription buffer [40 mM tris-HCl (pH 8.0), 6 mM MgCl₂, 100 mM NH₄Cl, 3 mM dithiothreitol (DTT), 0.16 mg/ml BSA, and 5% (v/v) glycerol] supplemented with a saturating concentration of the Pol III preparation, 400 μM CpU dinucleoside monophosphate, 10 U of RNasin, 50 μM each of CTP and UTP, and 4.6 μM [α-³²P]ATP (3000 Ci/mmol). The reaction mixture was incubated for 45 min at room temperature, and 20 μl of transcription buffer containing 2 mM each of all four NTPs was added to resume transcription. Transcription was continued for 2 s to 10 min in the presence or absence of pBS1100 competitor DNA and was terminated by addition of 40 μl of 20 mM EDTA. Samples were phenol-extracted, and RNA was precipitated with ethanol, dissolved in formamide sample buffer, and analyzed in 8% (19:1) polyacrylamide sequencing gels. For experiments with labeled DNA, early elongation complexes were formed under similar conditions with CTP, UTP, and ATP (150 μM each) and chased as noted above. Digestions with RNase A (1 mg/ml final concentration) were done in transcription buffer at 20°C for 10 min. Purified RNA was digested with RNase H (100 U/ml) in 40 mM tris-HCl (pH 8.0), 4 mM MgCl₂, and 1 mM DTT at 37°C for 20 min. The size distributions of radioactive RNA were quantified with a PhosphorImager.
29. W. A. Rees, R. W. Keller, J. P. Vesenska, G. Yang, C. Bustamante, *Science* **260**, 1646 (1993).
30. We thank D. Clark for comments on the manuscript. Support of research at the University of California, San Diego by a grant from the National Institute of General Medical Sciences is gratefully acknowledged.

13 August 1997; accepted 16 October 1997